JOURNAL OF AIRCRAFT
Vol. 33, No. 1, January–February 1996

Pressure Sensitive Paint in Transonic Wind-Tunnel Testing of the F-15

Robert M. Dowgwillo,* Martin J. Morris,† John F. Donovan,† and Michael E. Benne‡
McDonnell Douglas Corporation, St. Louis, Missouri 63166

The pressure sensitive paint (PSP) technique has been used to measure surface static pressures on a 4.7% scale F-15E model with complex store loadings during a high-speed wind-tunnel test. Successful employment of the technique required an integrated process of paint formulation, model preparation, test procedure, data acquisition, and data reduction. Testing a total of 107 different combinations of configurations and flight conditions has provided an invaluable database. The data have immediate qualitative utility as surface flow visualization. Details of the measured pressure distribution were readily correlated with specific geometric features of the model. Absolute accuracy, and hence, quantitative utility is determined presently by the paint calibration. The digital data can be processed readily by appropriate software to provide pressure distribution plots, pressure increments, and integrated loads. This test's combination of duration, variety of flight conditions and configurations, and quick data turnaround represent a milestone in the practical application of PSP in aerospace testing.

Introduction

UNDERSTANDING the flowfield about a modern fighter aircraft is a challenge. The ability of these aircraft to operate within a wide range of Mach number, angle of attack, sideslip, and Reynolds number provides for many flow phenomena. High levels of aerodynamic interaction occur among the various components because of geometrically complicated and compact aircraft configurations.

Depicted in Fig. 1, the U.S. Air Force/McDonnell Douglas Aerospace (USAF/MDA) F-15E Eagle is an especially complex configuration owing to its provisions for the air-to-ground mission. Operation at transonic speeds with a collection of conformal fuel tanks (CFT), stores, pylons, sensor pods, and missiles creates a complicated flowfield about the undersurface of the aircraft. This flowfield directly affects aircraft structural loads, drag, store carriage loads, and postrelease store trajectories.

To improve the understanding of this flowfield, data were sought that could provide extensive information for a comprehensive collection of flight conditions and store loadings. Some flowfield data were available from previous tests using conventional techniques. These techniques included water-tunnel flow visualization, surface oil flow, laser light sheet, cone probe surveys, and surface static pressure taps. However, these results were either too limited in scope or not applicable. While computational fluid dynamics (CFD) analyses could satisfy the need for extensive data, solutions for this application are costly and time consuming. The few applicable solutions obtained to date[1] have been devoted to assessments of CFD capability rather than the establishment of a flowfield database.

Acquiring additional data was greatly constrained by cost. Modification of the existing model to carry metric stores was estimated to cost at least twice the available budget. Building a new pressure model was prohibitively expensive.

Pressure sensitive paint (PSP) is a relatively new technology that offers an affordable means of acquiring surface static pressure measurements on complex geometries. PSP has transitioned from the laboratory environment to application on several major MDA aircraft programs.[2]

This article describes the practical application of PSP to acquire extensive surface static pressure measurements on the undersurface of a subscale model of the F-15E during a high-speed wind-tunnel test. The emphasis here is on the special instrumentation, equipment, and procedures needed to successfully employ the PSP technique. Data are presented to illustrate the features and capabilities of the technique. The first section provides a brief overview of the physical phenomena basic to the PSP technique. This is followed by descriptions of the test section setup and the components of the PSP measurement system. Then, the test procedure is outlined, followed by a description of the data reduction process. Typical calibrated images are presented along with examples of the data presentations available through postprocessing. Finally, general conclusions about the performance of the PSP technique are presented along with recommendations for improvements.

PSP Overview

The physical phenomena that are the basis for the PSP technique have been introduced and discussed by Morris et al.[3,4] and Kavandi et al.[5] Therefore, only a brief discussion will be presented here.

Pressure sensitive coatings contain probe molecules that luminesce with an intensity that can be related to the local surface pressure. When exposed to light of the proper wavelength, a probe molecule is promoted to an excited state by absorbing a photon of the appropriate energy. Photoluminescence is one mechanism by which the molecule can lose this excess energy and return to the ground state. For pressure sensitive coatings, the excess energy can also be absorbed by oxygen molecules in a process called dynamic quenching. This quenching is usually modeled by some variation of the Stern–Volmer[4] relation:

$$I_0/I = 1 + K_q P_{O_2} \tag{1}$$

where I is the luminescence intensity of the paint, I_0 is the

Received Feb. 26, 1995; revision received Aug. 1, 1995; accepted for publication Aug. 4, 1995.

*Senior Project Engineer, Aeromechanics Department. Senior Member AIAA.
†Principal Technical Specialist, Propulsion and Thermodynamics Department. Senior Member AIAA.
‡Principal Technical Specialist, Aerodynamics and Thermodynamics Laboratories. Member AIAA.

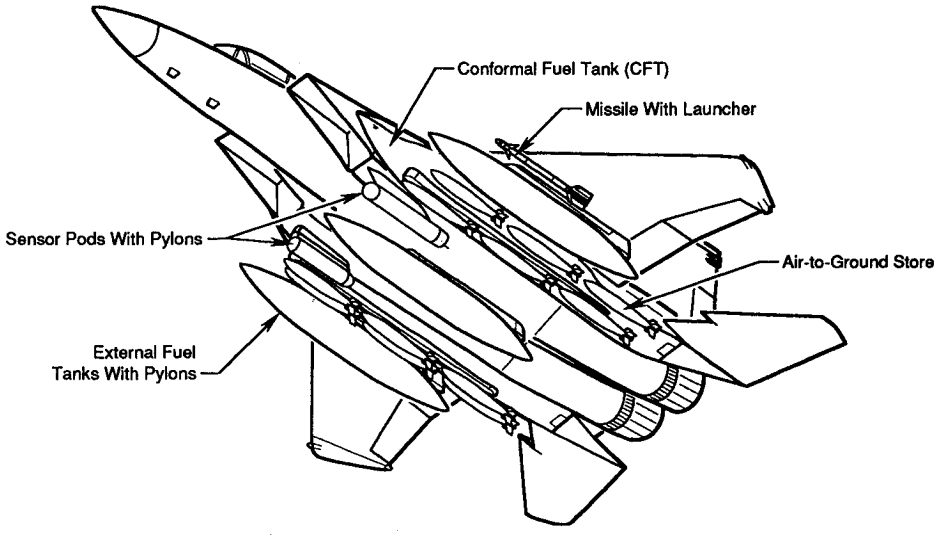

Fig. 1 F-15E with complex store loading.

luminescence in the absence of oxygen, P_{O_2} is the partial pressure of oxygen, and K_q is the Stern–Volmer constant. Thus, the intensity ratio is directly related to the partial pressure of oxygen, and hence, to the local absolute static pressure. Unfortunately, the pressure sensitive probe molecules have other mechanisms by which they can change energy state, the most significant of which is manifested as a sensitivity to temperature. Techniques for dealing with these temperature effects[4] are critical to the successful use of PSP.

Test Setup

The test was conducted in the MDA Polysonic Wind Tunnel (PSWT) using a 4.7% model of the F-15E. The intermittent, or blowdown operation of this tunnel was well suited to the frequent model configuration changes required for this test. The model is the standard aerodynamic force and moment model used for F-15 high-speed wind-tunnel testing.

Figure 2 illustrates the arrangement of the wind-tunnel test section. The locations of the cameras, lights, and model were chosen to provide as complete a view as possible of the CFT store loadings within the physical constraints of the test section. Consequently, the model was installed inverted, about 1 ft below the tunnel centerline. A dummy balance installed on an aft-entry sting supported the model.

Boundary-layer transition strips were installed on the major model components and the centerline tank. These strips consisted of rows of miniature epoxy cylinders. Following standard practice, no strips were installed on the stores, sensor pods, or missiles.

PSP System

The PSP system is made up of three components: 1) paint, 2) illumination source, and 3) a luminescence detector. A schematic of the PSP data acquisition system is shown in Fig. 3.

Paint

The paint was formulated to exhibit high sensitivity to pressure and a minimum sensitivity to temperature. Painting was a three-step process. First, the model surface was thoroughly cleaned with alcohol and lint-free cloths to remove all traces of dirt and oil. Then, a white primer layer was applied. After drying for 4 h, the primer was hand rubbed with lint-free cloths to achieve a smooth, uniform finish. Finally, the pressure sensitive layer was sprayed on with a modified commercial spray gun. The basic model was painted while fully assembled and mounted in the test section. The stores were painted individually. Drying time for the PSP layer was also 4 h. Target and alignment markings and luminescent reference dots were applied during the painting.

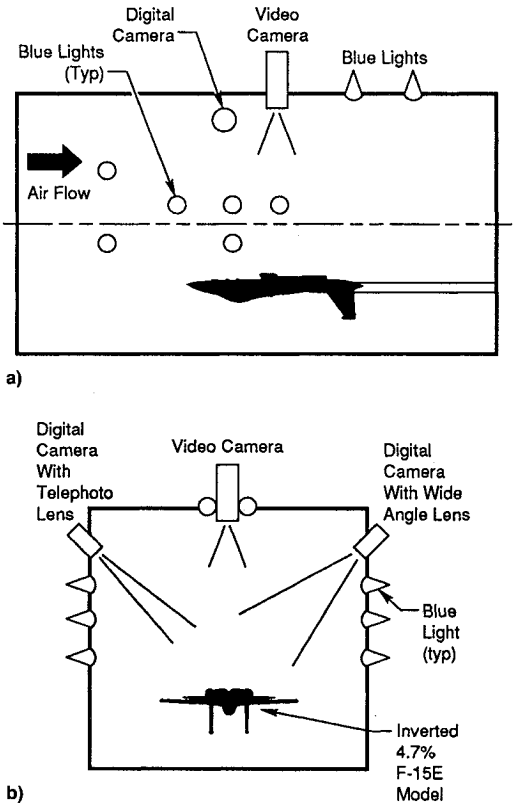

Fig. 2 Test section arrangement: a) sideview and b) view looking upstream.

The result was a rubbery, translucent yellow–orange finish. The paint must be smooth to avoid affecting the surface airflow. Runs or sags are unacceptable. If this condition exists, the paint must be removed and the process repeated. When applied properly, the paint layer is too thin to compromise the effectiveness of the boundary-layer transition strips.

A coupon containing a sample of the paint was prepared at the same time the model was painted. Subjecting this coupon to carefully controlled conditions in a pressure chamber

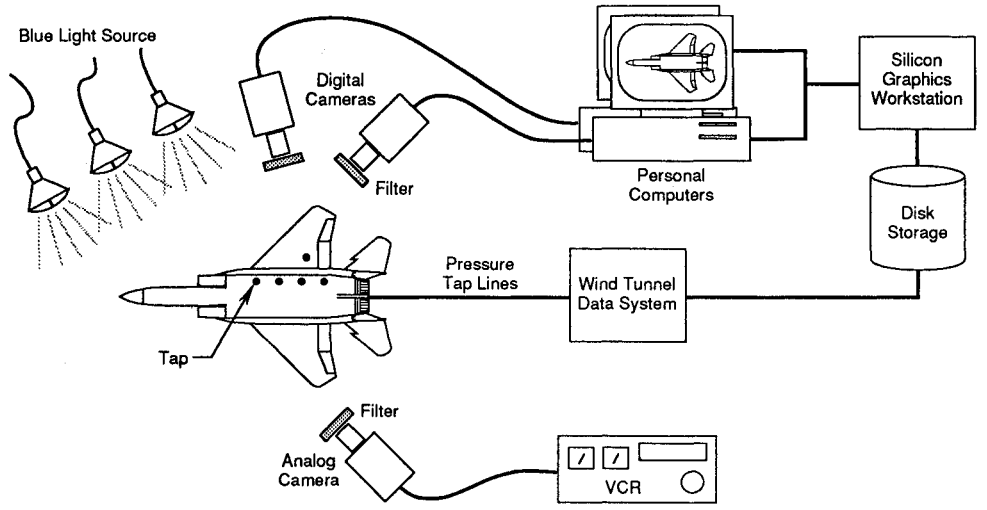

Fig. 3 Schematic of the PSP measurement system.

provided the laboratory calibration that forms the basis for subsequent data reduction.

Illumination Source

The illumination source was provided by low-voltage tungsten/halogen lamps. A filter stack was fitted to each lamp to produce a visible blue light. The visible light aided the lamp alignment while posing no hazard to personnel working in the test section. The lamps were air cooled. Fourteen lamps were distributed on the tunnel walls and ceiling to provide as uniform illumination as possible. The test section floor was painted matte black during this test to minimize unwanted reflections.

Luminescent Detectors

The luminescent detectors consisted of two digital cameras and a video camera. The digital cameras were the primary data source. They were equipped with scientific-grade charge-coupled device (CCD) arrays of 512 by 512 pixels. A good discussion of CCD arrays can be found in Ref. 6. The CCDs were cooled to minimize noise. They had a linear response with reasonably uniform pixel-to-pixel gain characteristics and a good dynamic range. Each camera was equipped with a 14-bit A/D converter.

The digital camera views are shown in Fig. 4. A wide angle lens on the right-hand camera provided an overall view of the model underside. To minimize data storage requirements, only that part of the camera field of view (FOV) that contained the model was recorded. This resulted in a rectangular image. A telephoto lens on the left-hand camera provided high spatial resolution data for the stores mounted on the forward and center CFT stations.

The digital images were captured on personal computers and transferred to a Silicon Graphics workstation for final processing.

The video camera was installed in the tunnel ceiling to provide an overall view of the model. The video camera was used to continuously monitor model and PSP behavior. The images were recorded on video tape.

Surface Static Pressure Taps

The only additional model instrumentation installed was five surface static pressure taps distributed on the lower surface. These taps provided in situ data for temperature effect compensation. Ideally, the taps are placed to provide a wide range of absolute static pressure while remaining within the FOV of at least one camera. The actual tap locations, indicated in Fig. 5, were further constrained by the limited space

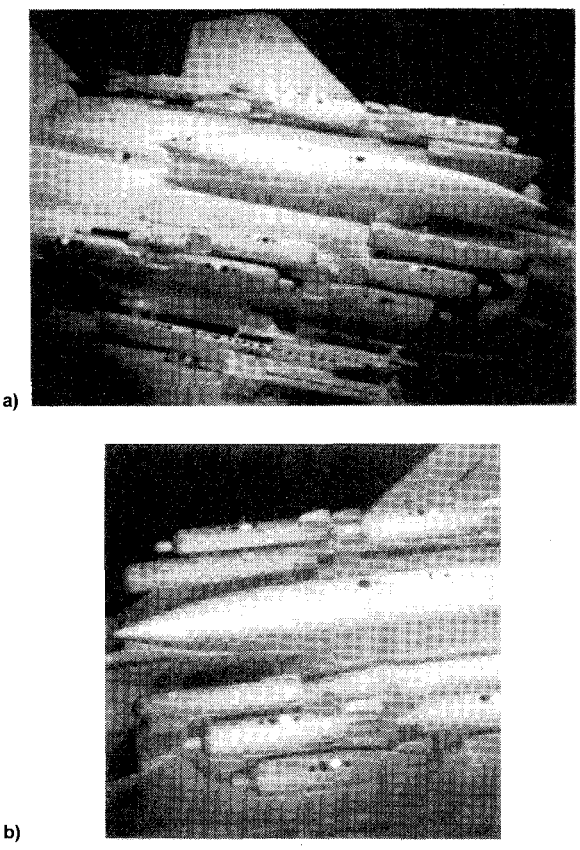

Fig. 4 Digital camera views: a) wide-angle and b) close-up images.

in the relatively small model for the necessary tubing. As a result, four of the five taps were installed in the left CFT, since it could be removed from the model for internal modification. The tubing is connected to the facility's standard pressure measurement system. The taps are protected during painting by blowing a steady stream of air back through the internal tubing and out the tap.

Test Procedure

The test was conducted in two phases. The first phase comprised independent variations in the freestream and engine inlet flow conditions for a baseline configuration. The variations included four angles of attack (0.7, 1.3, 3.5, and 7.0

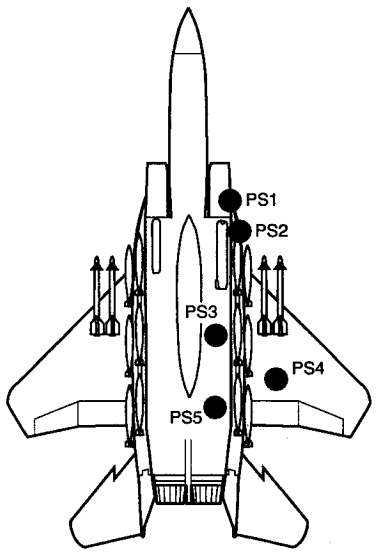

Fig. 5 Location of static pressure taps used for in situ calibration.

deg) two chord Reynolds numbers (6.2×10^6 and 9.4×10^6), four Mach numbers (0.60, 0.85, 0.95, and 0.98), and two inlet mass flow ratios (0.58 and 0.72). The second phase comprised systematic builddowns in configuration complexity. Starting with a complete, operationally relevant configuration, the changes in the surface pressure field were noted as model components were removed systematically. Twenty-five different configurations were tested over a narrow range of angle of attack at a constant Mach number.

Except for Reynolds number, the nominal test conditions were representative of F-15E flight at Mach = 0.95 and 5000 ft. Angle of attack ranged from 0.7 to 7 deg, corresponding to load factors of 0.5 to 6 g. The stabilator deflection was zero, the model setting closest to the range of actual stabilator deflections for trim. The inlet mass flow ratio was representative of maximum dry power. Nominal Reynolds number with respect to mean aerodynamic chord was 6.2×10^6. Nominal dynamic pressure was 1300 lb/ft^2.

A typical test run consisted of 1) taking prerun wind-off reference images, 2) starting the tunnel and establishing freestream conditions, 3) stepping in a pitch–pause sequence through up to four angles of attack, collecting PSP run images during a 3–5 s dwell at each angle of attack, 4) tunnel shutdown and taking postrun wind-off reference images. Camera exposure time was varied between 1–3 s, depending on the expected range of absolute pressures. The exposure time for a particular run was the same for the reference and run images.

The only special care taken with the PSP was to avoid oil contamination, since oil interferes with the oxygen-quenching mechanism. Latex gloves were worn to control paint contamination when working on the model. Isolated defects and scratches that accumulated during the many model changes did not compromise the data. However, over the course of many runs at high dynamic pressure, the paint on forward-facing surfaces collected dirt or eroded due to small debris in the flow. As needed, localized repairs to the paint were made at the end of the day. The entire model was repainted once during this test in order to maintain data quality. The paint can be readily peeled off. The primer is removed with isopropyl alcohol.

Because the model did not have a live balance, the normal closed-loop procedure of using measured model loads to correct angle of attack for sting deflection could not be used. Instead, an open-loop correction based upon balance loads measured during a previous test with this model at similar test conditions was devised.

A total of 107 different combinations of flight condition and configuration were tested among 39 runs. All of the data were collected within one week.

Data Reduction

The major data reduction task is the conversion of the images from luminescence intensity into absolute pressure.

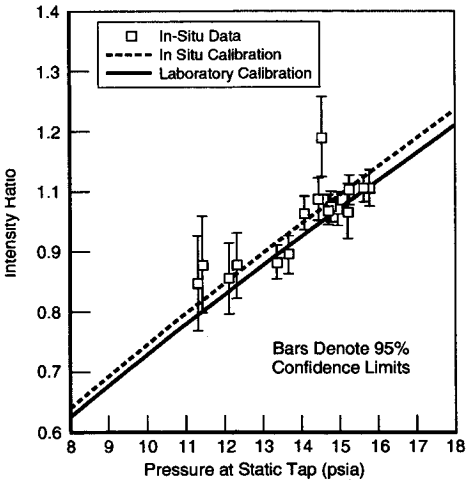

Fig. 6 Typical PSP calibration curves.

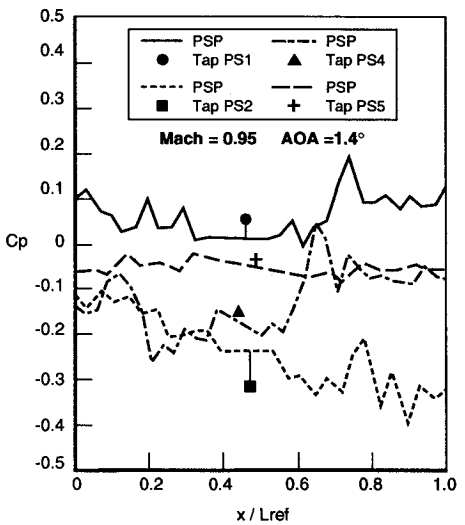

Fig. 7 Comparison of static pressure tap measurements with calibrated PSP data.

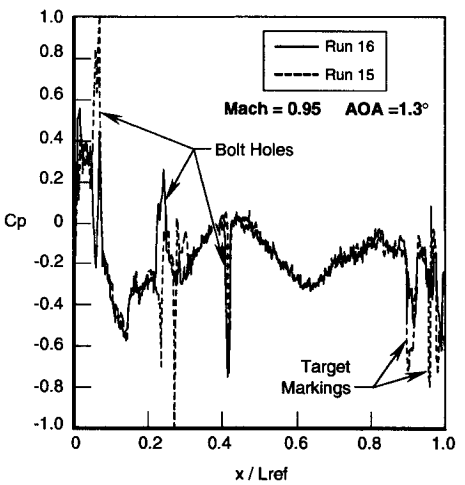

Fig. 8 Example of PSP data repeatability.

The following procedure was applied individually to the images collected by each camera at each angle of attack of a run. First, a dark image was subtracted from the reference and run images. A dark image is acquired by leaving the camera shutter closed during the same exposure as the reference and run images. The dark image accounts for the dark current and the built-in bias voltage of the CCDs. Next, the reference and run images are aligned to compensate for any residual movement of the model due to airloads.[7] With the images aligned, the ratio of the reference and run intensities at each pixel was calculated. This ratio was then applied against the paint calibration curve to give the absolute pressure associated with that pixel.

A preliminary data reduction using the laboratory calibration was completed within 30 min after each run. This short turnaround was required to assess data quality and to help guide the test. This represented a distinct improvement over previous tests with PSP.

If the reference and run images are taken with the model surface at the same temperature, the laboratory calibration would be adequate, since the intensity ratio effectively removes temperature effects. However, maintaining consistent, uniform temperature conditions was not possible for this test. The final data reduction, performed after the test, consisted of applying the intensity ratio data to an in situ calibration curve to compensate for the gross unknown temperature differences between the run and reference images. The calibration was obtained by applying a least-squares technique to shift the laboratory calibration curve to provide the best agreement with the surface static pressure tap data. A separate calibration curve was determined for each run using the tap data for all of the separate angle-of-attack points in the run. Figure 6 shows an example of the laboratory calibration curve, the pressure tap data, and the resultant in situ calibration curve.

Note that this technique compensates for gross, or average, temperature differences. Local temperature variations over the model surface are not considered. These variations are primarily controlled by the differences in thermal mass of different portions of the model, especially thin wing trailing edges. A complete accounting for surface temperature changes would require a global measurement of surface temperature. This would be supplied best by a temperature sensitive paint (TSP) used simultaneously with the PSP.

Data Quality

The primary measure of the data quality for this experiment was the five static pressure taps on the model surface. In

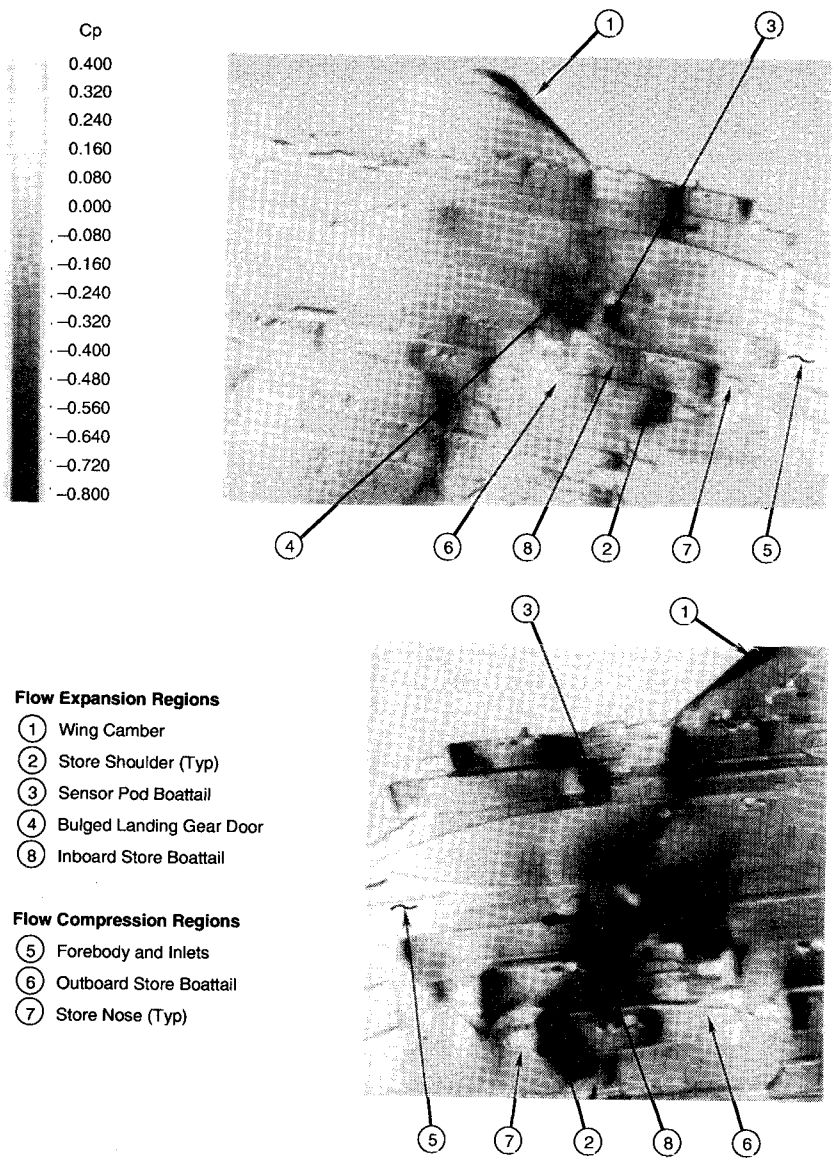

Fig. 9 Typical calibrated image pair from PSP data, Mach = 0.95, angle of attack = 1.4 deg.

addition, the qualitative features of the pressure distributions from similar test conditions were compared for repeatability.

The data from both the PSP and the pressure taps represent an average of the measurements made during the 1- to 3-s exposure of the digital cameras. The averaging of the PSP data was inherent to the operation of the CCDs. The tap pressures were sampled at 14 Hz and the average calculated.

Morris et al.[4] and Sabjen[8] describe the various sources of error that can affect PSP data quality. In practice, the data uncertainty for this test was determined by the quality of the in situ calibration. As shown in Fig. 6, the difference between the laboratory and in situ calibration curves was usually small, but not always negligible. The uncertainty bounds on the intensity ratio of the in situ data reflect the difficulty in defining the representative intensity ratio at each pressure tap location. This scatter is typical for these types of experiments and is the result of uncertainties due to large pressure gradients in the vicinity of some of the taps, local surface temperature variations, photometric errors, and the difficulty of locating the tap in the digital image. In this case, the uncertainty of the in situ calibration curve results in an uncertainty in absolute pressure of about ± 0.43 psia, to 95% confidence. This corresponds to an uncertainty of ± 0.045 in pressure coefficient.

Figure 7 shows a typical comparison of the local pressure distribution derived from the PSP data with simultaneous surface static pressure tap measurements made at four locations on the model. Each PSP pressure distribution was created by cutting the PSP image along a line about 1 in. long passing through the tap location. The comparison is good, considering that the tap data are an average over a small but distinct area, and the presence of the tap precludes actually having PSP data at the tap location. Spurious PSP data due to the image of the pressure tap have been removed. The sawtooth behavior of the data is principally due to pixel-to-pixel variation in the CCD gain. If desired, this behavior can be minimized by spatial averaging.

Figure 8 demonstrates the repeatability of PSP data by comparing a pressure distribution along a buttline cut on the model surface for two separate runs with the same configuration and freestream conditions. The cut extended from just aft of the inlet lower lip to just beyond tap PS3, a distance of about 12 in. on the model. The data compare well. The isolated spikes are the result of unpainted screw heads and markings on the paint. Normally, these would be edited out. Again, the sawtooth behavior is typical of this test.

Typical PSP Results

Acquiring the PSP images in a digital format provides unlimited options for postprocessing. This section will illustrate the kinds of data presentations that have been developed.

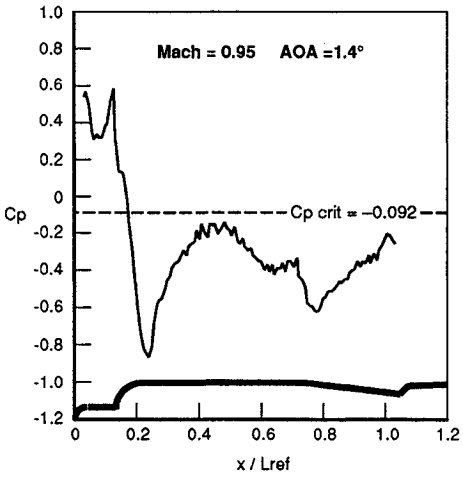

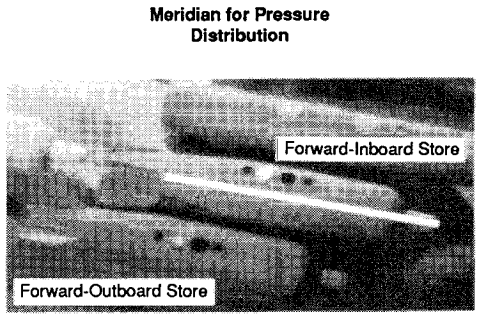

Fig. 10 Pressure distribution along meridian on left forward–inboard store, F-15E + LANTIRN pods + 4 AIM-9 missiles + 10 stores.

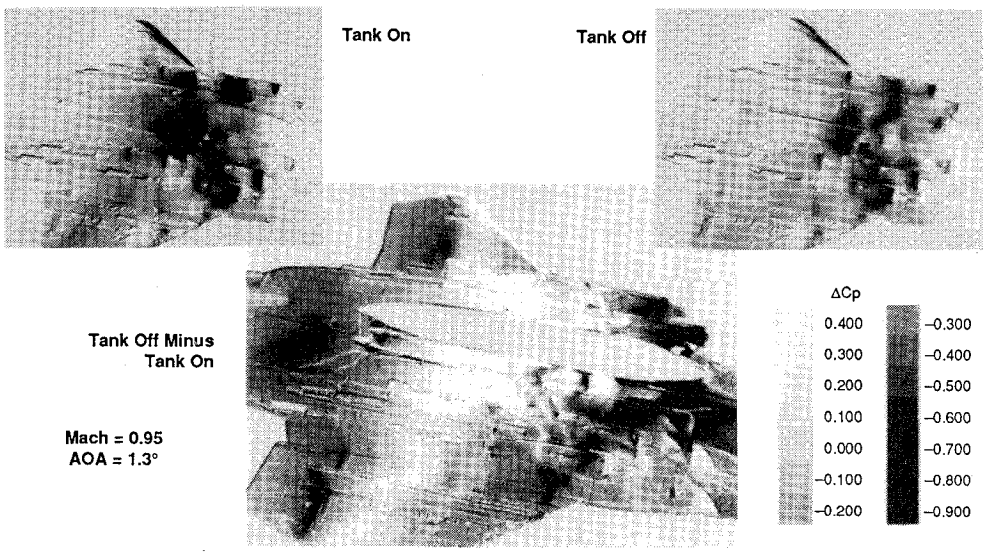

Fig. 11 Change in surface static pressure caused by removing centerline fuel tank.

Figure 9 is an example of surface static pressure data derived from the PSP images. The data have been gray scaled according to local pressure coefficient. The gray scale is used here only as a convenience for publication. Normally, the pressures are rendered in false color, which provides a more effective presentation.

As indicated in the figure, the variations in pressure can be correlated readily with specific geometric features of the model. Distinct regions of low pressure (i.e., negative pressure coefficient) include the blunt shoulders of the forward-mounted CFT stores, the boattail of the sensor pod, the bulged main landing gear doors, and the wing conical camber. Regions of high pressure (i.e., positive pressure coefficient) include the noses of the stores, the engine inlets, and the boattail of the forward–outboard stores. The reader may find the black-and-white images of Fig. 4 helpful in identifying the model components.

Each pixel of a PSP image is, in effect, a separate pressure measurement. Thus, the number of pressure measurements on any particular model component is determined by the number of pixels covering the image of the component. In this case, the wide-angle image provides about 1200 pressure measurements/in.^{2} on the model. The telephoto image provides about 3600 measurements/in.^{2}.

Figure 10 presents the surface pressure distribution along a meridian of the left forward–inboard store in the wide angle image of Fig. 9. The details of the pressure distribution correlate directly with the shape of the store. Note that L_{ref} is an arbitrary reference length used to nondimensionalize the position on the model. Here, L_{ref} is the length from the nose to the root leading edge of the tail fins of the store. Comparison with the critical pressure coefficient $C_{p\,\text{crit}}$, for these test conditions shows there is extensive supersonic flow.

A data presentation that highlights changes in the pressure field is particularly useful when assessing the relative contributions of different model components to the flowfield. Figure 11 presents an image of the pressure change caused by the removal of the centerline fuel tank. This image is created by subtracting the image with the fuel tank off from the image with the fuel tank on. This subtraction is done simply on a pixel-by-pixel basis. It is immediately seen that the pressures on the forward stores are little affected, while those on the midstores are changed significantly. The ghost image of the tank itself has been masked to avoid confusion. This presentation is invaluable for assessing the sensitivity of the flowfield to the presence of particular model components.

The most recent postprocessing development is the ability to map the two-dimensional PSP pressure images onto a three-dimensional surface grid. This allows the PSP data to be analyzed using the sophisticated tools developed for CFD postprocessing.

A detailed description of the mapping procedure can be found in Donovan et al.,[7] but a brief description is given here. The procedure is illustrated in Fig. 12. First, the image coordinates of targets placed on the model are determined. The model coordinates of these points are assumed to be known. Using both the image and model coordinates of these target points, the location and orientation of the camera relative to the model coordinate system are calculated (six parameters). This information plus the camera lens focal length now define a transformation between the model and the image. The previously generated grid defines points where the pressure is desired on the surface of the model. Each point is projected into the image using the transformation defined. In the image a bilinear interpolation is used to determine the pressure at each grid point based on the surrounding pixels. The result is a grid that defines the model surface with a pressure assigned to each grid point.

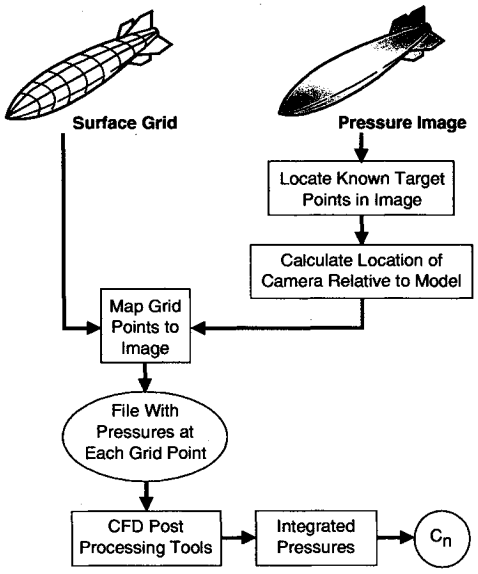

Fig. 12 Mapping process.

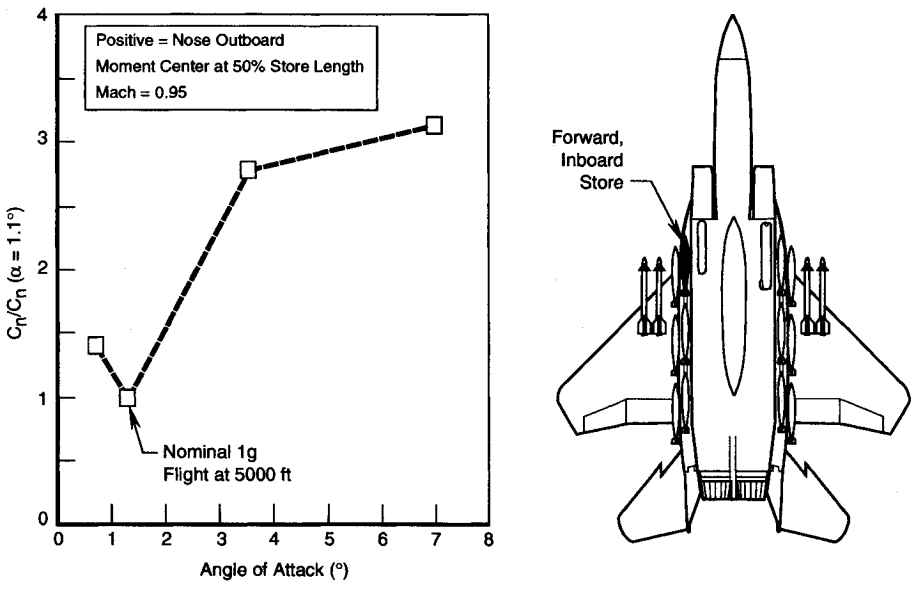

Fig. 13 Normalized yawing moment coefficient vs for store at forward–inboard CFT station vs angle of attack.

In the present case, the mapped PSP pressures for selected stores were integrated using a standard CFD postprocessing program to derive a measure of the store carriage loads from the surface pressures provided by PSP. Figure 13 shows normalized yawing moment coefficient, derived from the PSP images of the forward–inboard store, as a function of angle of attack. It is not possible to calculate an absolute yawing moment, since pressure data are not available for the portion of the store facing the aircraft. While a direct comparison with a metric model was not possible, these results suggest that the store yawing moment increases with angle of attack, probably due to an increase in local sidewash.

Conclusions and Recommendations

The PSP technique has been successfully employed in a high-speed wind-tunnel test to provide extensive surface pressure measurements on a tactical fighter configuration with complex store loadings. This test's combination of configuration complexity, duration, and data processing capabilities represents a milestone in the practical application of the PSP technique.

The data have immediate qualitative utility as surface flow visualization. The data showed excellent correlation with the geometric features of the model configuration. The high data density enabled even subtle effects to be detected.

For quantitative use, the in situ calibration suggested that the PSP data agreed with the pressure tap data to ± 0.43 psia to a 95% confidence level. This corresponds to a pressure coefficient of about ± 0.045. This is consistent with previous PSP tests performed with this system.

In practice, the absolute accuracy of the PSP system described here was determined by the quality of the in situ calibration used to compensate for temperature differences between wind-off and wind-on conditions. The limiting factors are 1) the uncertainty in defining the intensity ratio associated with the static pressure tap measurement and 2) the spatial temperature variation over the surface of the model. The first factor can be reduced with more sophisticated interpolation methods. The second factor requires a simultaneous, global measurement of model surface temperature, such as that provided by TSP. However, the spatial temperature variation is considered mostly a secondary effect in this test. The area of greatest interest was the center fuselage, which has a high thermal mass and is least affected by the temperature variations during the 20-s run time of the tunnel. Moreover, the high conductivity of the aluminum and steel model tends to even out any large surface temperature changes. The development of PSP with no temperature sensitivity at all could reduce the dependency on in situ calibrations. Incorporation of the in situ calibration in the initial data reduction with even shorter turnaround times is desirable for exploratory tests like this one.

The large variety of cases tested has provided an invaluable database on the transonic flowfield on the undersurface of the F-15E. These data are particularly useful for establishing the sensitivity of the flow to aircraft store loading and flight condition. This information has already contributed to the efficient employment of CFD to study these flows.

This test demonstrated that the PSP technique has matured into a cost-effective flow diagnostic tool. The authors know of no other technique, experimental or computational, that could provide such extensive surface pressure measurements for so many cases within the period of the test, at any cost. The technique should be seriously considered when extensive surface pressure measurements are needed.

Like CFD, the large amounts of data generated by the PSP technique demand special postprocessing tools for effective presentation and interpretation of the results. Fortunately, having digital data offers considerable freedom in developing these tools. In particular, techniques should be developed that can map the entire PSP image to a surface grid of the complete model configuration. This would allow PSP data to be processed with many of the same tools used for CFD.

Acknowledgments

This wind-tunnel test was supported by the U.S. Air Force F-15 System Project Office, under Contract F33657-91-C-2002, P00014. Gina Manfra was the Monitoring Officer. The PSP system was developed under McDonnell Douglas Independent Research and Development activities.

References

[1]Fox, J. H., Donegan, T. L., and Jacocks, J. L., "Solution of the Euler Equations Modeling the Flow Field Produced by an F-15E with Stores at a Mach Number of 0.98," Arnold Engineering and Development Center, AEDC-TR-89-13, Nov. 1989.

[2]Crites, R. C., Benne, M. E., Morris, M. J., and Donovan, J. F., "Optical Surface Pressure Measurements: Initial Experience in the MCAIR PSWT," *Wind Tunnels and Wind Tunnel Test Techniques*, The Royal Aeronautical Society, Southampton Univ., UK, Sept. 1992 (Paper 12).

[3]Morris, M. J., Donovan, J. F., Kegelman, J. T., Schwab, S. D., Levy, R. L., and Crites, R. C., "Aerodynamic Applications of Pressure-Sensitive Paint," AIAA Paper 92-0264, Jan. 1992.

[4]Morris, M. J., Donovan, J. F., Benne, M. E., and Crites, R. C., "Aerodynamic Measurements Based on Photoluminescence," AIAA Paper 93-0175, Jan. 1993.

[5]Kavandi, J., Callis, J., Gouterman, M., Khalli, G., Wright, D., Green, E., Burns, D., and McLachlan, B., "Luminescent Barometry in Wind Tunnels," *Review of Scientific Instruments*, Vol. 61, No. 11, 1990.

[6]Anon, "Charge-Coupled Devices for Quantitative Electronic Imaging," 1991 Photometrics Ltd., 1991.

[7]Donovan, J. F., Morris, M. J., Pal, A., Benne, M. E., and Crites, R. C., "Data Analysis Techniques for Pressure and Temperature Sensitive Paint," AIAA Paper 93-0176, Jan. 1993.

[8]Sabjen, M., "Uncertainty Estimates for Pressure Sensitive Paint Measurements," *AIAA Journal*, Vol. 31, No. 11, 1993, pp. 2105–2110.